A lab-on-a-chip for spectrophotometric analysis of biological fluids

G. Minas,[a] R. F. Wolffenbuttel[b] and J. H. Correia[a]

Received 13th May 2005, Accepted 18th August 2005
First published as an Advance Article on the web 22nd September 2005
DOI: 10.1039/b506817g

This paper reports a lab-on-a-chip for application in clinical analysis, especially in the spectrophotometric analysis of biological fluids. It is composed of three parts: (1) a microfluidic system die containing the microchannels fabricated using SU-8 techniques; (2) an optical filtering system based on highly selective Fabry–Perot optical resonators using a stack of CMOS process compatible thin-film layers; (3) a detection and readout system fabricated in a CMOS microelectronic process. The system enables low-cost and selective measurement of the concentration of several biomolecules in biological fluids. Operation is based on optical absorption in a well-defined part of the visible spectrum, defined by the reaction of a specific reagent with a specific biomolecule. Signals proportional to the intensity of the light transmitted through the biological fluid are available at the output in the form of bit streams, which allows simple computer interfacing. Moreover, the optical filtering system enables the measurement using white light illumination, thus avoiding the use of a wavelength dependent light source. This characteristic makes the lab-on-a-chip portable and ensures that the analysis can be performed at any location with instantaneous results, without the use of complex and expensive analysis systems. The quantitative measurement of uric acid and total protein in urine is demonstrated.

1. Introduction

For disease prevention, diagnostic and treatment patients are often subjected to biochemical analyses of their biological fluids. Usually, the analyses are carried out in clinical laboratories and the results become available after several hours, sometimes days. As a consequence a reliable diagnosis cannot be performed within the consultation time.[1] The need for rapid and on-line measurements with low sample volumes has led to the development of microsystems with the fluidic, detection and readout systems integrated in a single chip. The advantages associated with shrinking clinical analyses systems include: reduced sample size, higher degree of integration and hence enhanced potential for automation, shortened response time, potential for improved analytical performance, reduced laboratory safety and costs.[2,3]

In clinical diagnostics, the spectrophotometric analysis by optical absorption is one of the most commonly used analytical techniques for determining the concentration and/or amount of a particular biomolecule in biological fluids samples.[4] However, many of the analytes of interest for clinical analysis do not have chromophores that absorb light in a useful part of the visible range, and, consequently, the absorption can not be measured directly. Specific chemical reactions are available (reagents) to transform these analytes into colored products.[5] These colored products have an absorption maximum at a specific wavelength. This absorbance value is directly proportional to the concentration of the analytes in the samples.

The application of the particular lab-on-a-chip presented here is the spectrophotometric analysis of biological fluids, especially the colorimetric measurement, by optical absorption of the concentration of biomolecules in those fluids. This device should have the same reliability and precision of the spectrophotometric automated equipment used in the state-of-the-art clinical analyses laboratories[6] and, at the same time, it should feature the portability, cost and patient comfort of the reagent strips used for qualitative color readout.[7]

2. Lab-on-a-chip design

2.1 Lab-on-a-chip concept

The lab-on-a-chip combines in a multichip module the microfluidic system (see Fig. 1a), the optical filtering system (see Fig. 1b) and the detection and readout system (see Fig. 1c). The optical detection microsystem avoids the need for expensive readout optics and may enable low-cost disposable devices, which would improve the use of spectrophotometric analysis in clinical diagnostics.

The lab-on-a-chip operation is based on topside illumination with a white light beam that is transmitted through the microchannels containing the samples to analyze. The impinging light transmitted through the fluid is filtered, by the optical filters, to a narrow spectral band centered at the wavelength at which the colored mixture has its absorption maximum. The intensity of the selected spectral component is measured using underlying photodetectors. This optical intensity is proportional to the biomolecule concentration. A light-to-frequency converter is integrated with the photodetectors to convert the analog signal into a digital signal.

[a]*University of Minho, Dept. of Industrial Electronics, Campus de Azurém, 4800-058, Guimarães, Portugal.*
E-mail: gminas@dei.uminho.pt; higino.correia@dei.uminho.pt;
Fax: +351 253 510189; Tel: +351 253 510190
[b]*Delft University of Technology, Fac. EEMCS, Dept. ME, Mekelweg 4, 2628, CD Delft, The Netherlands.*
E-mail: r.f.wolffenbuttel@ewi.tudelft.nl

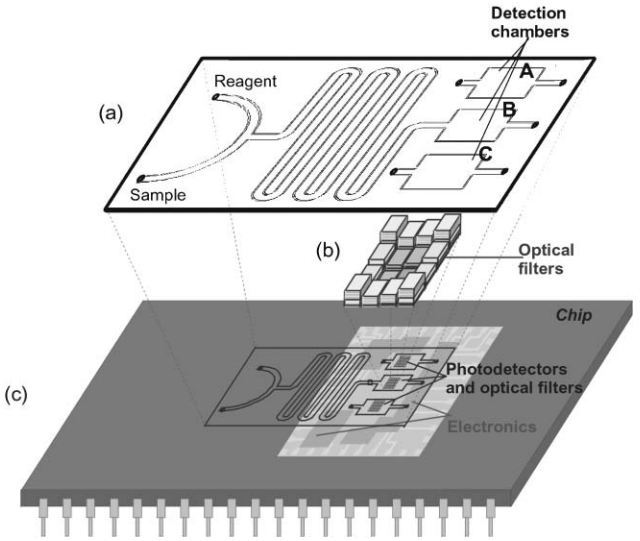

Fig. 1 Artist impression of the lab-on-a-chip structure.

Shrinking of clinical analysis systems is fundamentally limited by the amount of biomolecules available in the sample volume (*i.e.* the product of the cross-sectional area of the channel and the illuminated channel length) and thus by the concentration of the desired analyte. Albumin in urine is the protein that has the lowest target molecules (on average 1 μmol l^{-1}) and also the lowest concentration (less than 15 mg dl^{-1}). For a 5 mg dl^{-1} concentration of albumin in urine there are 3.35×10^5 biomolecules per picoliter (enough for reproducible measurements of analyte concentrations[8]). Whether actual shrinking to the picoliter range is feasible also depends on practical aspects, such as the channel height required to achieve measurable absorption (which depends on the biomolecules absorption coefficient (α), for example, $\alpha = 0.27$ m^{-1} for an albumin concentration of 5 mg dl^{-1} and $\alpha = 54.97$ m^{-1} for a uric acid concentration of 5 mg dl^{-1} (see ref. 9 and 10)), as well the minimum channel width and the diode area, which are both set by lithographic constraints. The typical minimum dimension for the channel height is 500 μm.

2.2 Microfluidic system

The microfluidic system contains the microchannels and the detection chambers (see Fig. 1a). Each detection chamber is 2 mm wide, 3 mm long and 500 μm deep. The high depth is crucial for the optical absorption measurements. The detection chamber, A, contains the reagent and is needed to obtain the baseline reference and to calibrate the light source. The detection chamber, B, allows the colored mixture analysis. The detection chamber, C, is needed to calibrate the biomolecule concentration (with a well-known concentration standard) and also to compensate the white light oscillations. The main channel is 500 μm wide, 70 mm long and 500 μm deep, with a liquid volume quantity of 20 μl. A computer simulation, described in ref. 11, has been carried out to derive the appropriate design layout criteria for a complete and homogeneous mixing of the reagent with the sample.

2.3 Optical filtering system

The Fabry–Perot optical filter allows the use of only a white light source for illumination and should be designed to yield a narrow passband around the wavelength for which the colored mixture has its absorption maximum. This characteristic enables the selective measurement of the light intensity, at the desired wavelength, transmitted through the mixture. The Fabry–Perot optical filter consists of two parallel mirrors with a resonance cavity in the middle. The thickness of the resonance cavity determines the tuned wavelength. The mirrors are dielectric mirrors that offer high performance characteristics (high reflectivity with low absorption losses).[12] These features enable high-selectivity, which makes the lab-on-a-chip broadly applicable.

The dielectric mirrors are composed of a stack of TiO_2 and SiO_2 thin-films (materials with high and low refractive index, about 3.0 and 1.5, respectively). SiO_2 has been selected because of the IC process compatibility and the fact that the wavelength dependence of its refractive index for the spectral band between 480 nm and 700 nm is almost constant (1.465 to 1.457, respectively). Also TiO_2 has been selected for IC process compatibility. Moreover, the deposition process is well-characterized. Rather than just one optical filter, a 16 optical filter array has been developed. The complete 4×4 array (Fig. 1b) allows the quantification of the concentration of 16 different biomolecules with the same device. Table 1 presents those biomolecules. The wavelengths at which each colored mixture has its maximum of absorbance are closely spaced (8 nm on average). Therefore, and for broadly applications, the Fabry–Perot optical filters must be highly selective; their FWHM (Full-Width-Half-Maximum) should be less than 6 nm to avoid misidentification in the analysis by possible overlapping of absorbance spectra of mixtures.

A thin-film optics software package (TFCalc 3.4) was used for the structural optimization of the optical filters. Simulation results show that a multilayer stack (5 layers) of TiO_2/SiO_2 thin-films for the dielectric mirrors and a SiO_2 layer for the cavity (see Table 1) is a highly suitable option for the optical filters in terms of optical characteristics, feasibility and fabrication process. The simulated transmittances for all 16 Fabry–Perot optical-channels allows the conclusion that each of the channels is sensitive to a single spectral band, with FWHM < 6 nm. Furthermore, the ratio between the transmitted peak and the baseline is larger than 3.5 and peak transmittance is higher then 86%. A commercially available passband optical filter on the top of the lab-on-a-chip is used to avoid transmission of the non-visible part of the spectrum.

2.4 Detection and readout system

The photodetectors convert the light intensity that is transmitted through the colored mixture into a photocurrent. They are *pn*-junction photodiodes, fabricated using the *n*+/*p*-epilayer junction available in a CMOS process, without additional masks or steps. The two oxide layers that result from the CMOS process on top of the *pn*-junction, were removed (without affecting the CMOS process) to eliminate the wavelength dependence of the transmission through these

Table 1 The 16 biomolecules that can be analyzed in the optical lab-on-a-chip and the corresponding layers materials and thickness for the 16 Fabry–Perot optical filters array

Biomolecule		17-Ketosteroids	Chlorine	Uric acid	Cholesterol	Glucose	Magnesium	Creatinine	Urea	Hemoglobin	Beta glucuronidase	Bilirubin	Leucine aminopeptidase	Calcium	Oxalate	Total protein	Albumin
Absorption maximum/nm		480	488	495	503	512	520	528	536	544	552	560	568	575	583	591	600
Filter number		1	2	3	4	5	6	7	8	9	10	11	12	13	14	15	16
	Layer	Material	Thickness of each layer/nm														
Mirror	1	TiO_2	45	45	45	45	45	45	45	45	45	45	45	45	45	45	45
	2	SiO_2	95	95	95	95	95	95	95	95	95	95	95	95	95	95	95
	3	TiO_2	45	45	45	45	45	45	45	45	45	45	45	45	45	45	45
	4	SiO_2	95	95	95	95	95	95	95	95	95	95	95	95	95	95	95
	5	TiO_2	45	45	45	45	45	45	45	45	45	45	45	45	45	45	45
Cavity	6	SiO_2	140	146	152	158	164	170	176	182	188	194	200	206	212	218	224	230
Mirror	7	TiO_2	45	45	45	45	45	45	45	45	45	45	45	45	45	45	45	45
	8	SiO_2	95	95	95	95	95	95	95	95	95	95	95	95	95	95	95	95
	9	TiO_2	45	45	45	45	45	45	45	45	45	45	45	45	45	45	45	45
	10	SiO_2	95	95	95	95	95	95	95	95	95	95	95	95	95	95	95	95
	11	TiO_2	45	45	45	45	45	45	45	45	45	45	45	45	45	45	45	45

[a] Note: Some of the colored mixtures have not only a single wavelength for its maximum of absorbance (peak), but a wavelength range.[5] In that case, the wavelength has been selected that simplifies the filter fabrication.

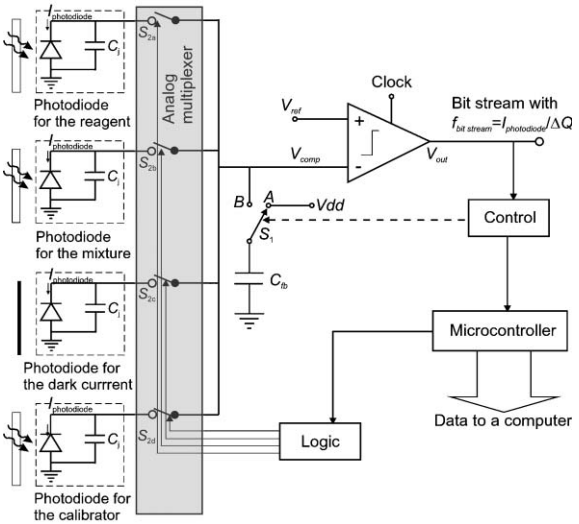

Fig. 2 Block diagram of the photodiode readout circuit. The comparator is a clocked high-speed regenerative comparator with a rail-to-rail input circuit. A dark current compensation channel is implemented with a photodiode completely covered with metal.

layers. The first oxide layer should remain to protect the photodiode active area.[10]

A light-to-frequency converter is integrated with the photodiodes (see Fig. 2). Its output frequency is a function of the charge change in the capacitors, ΔQ, which is proportional to the input photocurrent.[13] Therefore, this circuit provides a digital output signal with a frequency proportional to the light transmitted through the colored mixture. This digital value is then collected by a microcontroller, which makes the calculations, based on Lambert–Beer's law, to obtain the biomolecule concentration. The microcontroller also combines data, makes decisions, controls ranges in the photodetectors and provides a standardized output format for higher computer levels.

3. Lab-on-a-chip fabrication

3.1 Microfluidic system

Fig. 3 shows a photograph of the microchannels fabricated using a layer of photoresist SU-8 deposited on the glass substrate, which gives the required low sidewall roughness and deep rectangular vertical profile of the microchannels (suitable for optical absorption measurement). The SU-8-based

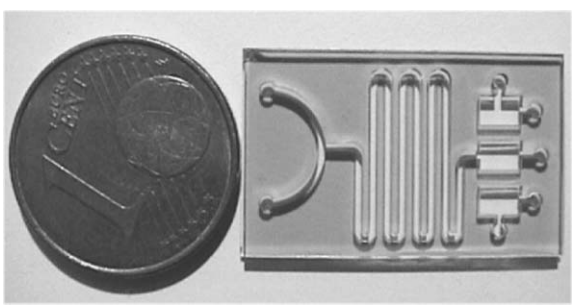

Fig. 3 A photograph of the SU-8-based structure microchannels.

fabrication is a low-cost process, UV lithography semiconductor compatible and does not require expensive masks, a regular transparency foil, like the one used in printed circuit boards, is enough. It can be processed with a spincoating and UV maskaligner.[14] In addition, the microfluidic system can be a disposable die, which minimize the cost associated with cleaning of the microchannels and avoids the contamination between analyses.

3.2 Optical filtering and detection system

The Fabry–Perot optical filters array is fabricated using CMOS-compatible post-processing on top of the photodiode array. Films are deposited by Ion Beam Deposition from high purity Ti and SiO_2 targets. The relative deposition non-uniformity is 2% on an area of 10 cm^2.[15]

The filter fabrication starts with the deposition of a 45 nm TiO_2 layer over the entire array, after completion of the CMOS process. Subsequently, the layers 2 to 5 are deposited again over the entire array (the thickness of each layer is described in Table 1). In subsequent deposition steps, for which a mask is used and each of them with a different deposition time (see Fig. 4), the 6th SiO_2 layer is deposited in a total thickness ranging between 140 nm and 230 nm in 6 nm steps, forming the filters number 1 to 16. Each mask is used during a deposition time, $2^{(n-1)}$ t (n is the mask number), which results in the 2^n different thickness of the 6th SiO_2 layer. After completion of the 16 thickness of the 6th layer, the top mirror is formed by deposition of layers 7 to 11 over the entire array. Fig. 4(e) shows a photograph of the cross-section of one of the optical channels. The 16 Fabry–Perot optical filters array fabrication requires only 4 masks and 15 deposition steps. The optical filters can be easily tuned to different spectral bands by adjusting only the thickness of the 6th layer, without affecting the lab-on-a-chip layout.

The CMOS compatible photodetectors and readout circuits have been fabricated through a double-metal, single-polysilicon, 1.6 μm n-well CMOS process (see Fig. 5). The microfluidic system is glued to the optical detection microsystem chip. The CMOS chip and the filtering system are the same for several analyses of the 16 biomolecules.

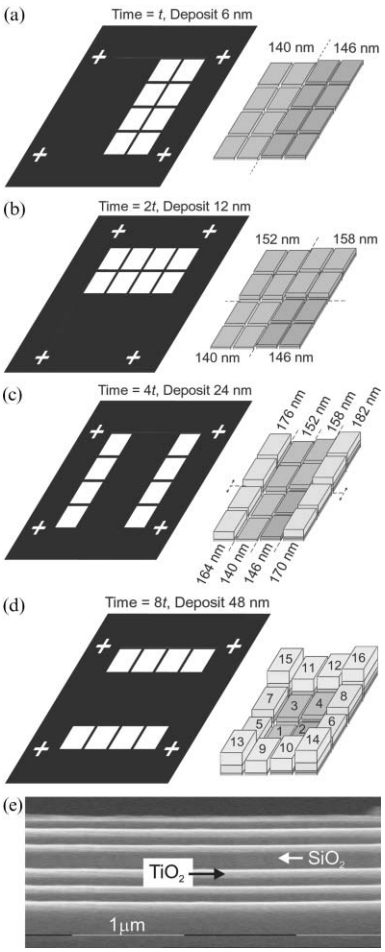

Fig. 4 The deposition process of the SiO_2 layer 6. The crosses are alignment marks. (a) Applying the 1st mask, two different SiO_2 thicknesses are obtained; (b) applying the 2nd mask, 4 different SiO_2 thicknesses are obtained; (c) applying the 3rd mask, 8 different SiO_2 thicknesses are obtained; (d) applying the 4th mask all the 16 SiO_2 thicknesses are obtained (the numbers show the position of each filter in the array); (e) SEM photograph showing the cross-section of the Fabry–Perot optical filter number 3.

4. Experimental results

Proper operation of the lab-on-a-chip is confirmed using a set of experiments that involve the quantitative measurement of uric acid and total protein in urine.[16,17] Three levels are distinguished. First, the optical performance of the biomolecules is evaluated using macroscopic laboratory equipment (section 4.1). Subsequently, the opto-electric performance of the lab-on-a-chip is characterized, followed by the quantitative measurement of uric acid and total protein in urine (section 4.2).

4.1 Measurements on well-known standards

To design and calibrate the detection and filtering system, some measurements on well-known uric acid and total protein standards need to be performed for determining the real transmitted wavelengths and the actual relationship between the biomolecule concentration and the intensity of the

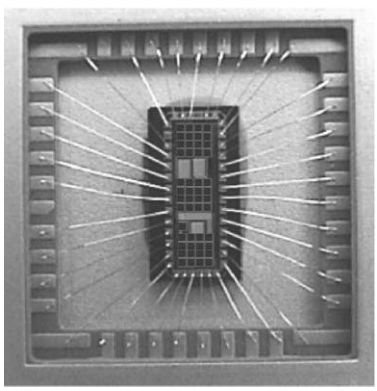

Fig. 5 A photograph of the fabricated optical detection microsystem. The area of each optical channel is 200 × 200 μm^2 and the die area is 2.0 × 5.3 mm^2.

Table 2 Result of linear fit from absorbance calibration plot measured with well-known biomolecule standards and performed in a state-of-the-art spectrophotometer

Analytes (measured conc. range/mg dl^{-1})	$\lambda_{(absorption\ maximum)}$/nm	Linear conc. range/mg dl^{-1}	Slope/(arb. units) dl mg^{-1}	Intercept (arb. units)	Correlation coefficient (R^2)
Uric acid (0–120)	495	0–30	$(3.7 \pm 0.1) \times 10^{-3}$	$(0.9 \pm 0.8) \times 10^{-3}$	0.99957
Total protein (0–100)	592	0–100	$(2.00 \pm 0.03) \times 10^{-4}$	$(-5.1 \pm 0.8) \times 10^{-4}$	0.99992

[a] Note: The $\pm$ values are $\pm$ one standard deviation.

transmitted light. It was also considered necessary to verify whether the use of small quantities of samples remains compatible with the prescribed procedures that are described in the reagent protocol, which are based on 3 ml of sample volume. So, the sensibility, the linearity and the reproducibility coefficient variation should not be changed. All the measurement values that will be presented are the mean of 10 replicate determinations. The measurements described in this section were performed with a 200 µl sample volume in a 1 mm lightpath cuvette and with a model UV-3101PC SHIMADZU spectrophotometer. The reagents used in the measurements of the uric acid and total protein in urine are the "Infinity™ uric acid reagent, procedure n. 684" and the "Microprotein-PR, procedure n. 611", respectively, both from Sigma-Aldrich.[5] They react with a sample of urine in a 50:1 ratio, and produce an absorption maximum at $\lambda = 495$ nm (for uric acid) and at $\lambda = 592$ nm (for total protein). Measurements were performed comprising the range of normal and typical abnormal analyte concentration values in a human being. The data was read and analyzed using a least squares program to perform a linear regression for determining the two linear coefficients: the slope and the intercept (value at the origin). Table 2 presents these values and their deviations.

The following conclusions can be drawn from those measurements. First, the uric acid analysis presents a linear behavior for concentrations as large as 30 mg dl^{-1} (for higher concentrations the sample should be diluted and re-assayed multiplying the result by the dilute factor). The total protein presents a linear behavior for all the measured concentrations. Second, the intensity of the color produced by the mixture is directly proportional to the biomolecule concentration, once it obeys Lambert–Beer's law. Third, the uric acid and the total protein absorption spectra show a maximum peak at the wavelength $\lambda = 495$ nm and $\lambda = 592$ nm, respectively, both with FWHM = 90 nm. Fourth, the reproducibility mean coefficient variation of 10 replicate analyses for each concentration was 6% and 9% for the uric acid and for the total protein, respectively. For both analyses, it can be concluded that the reduction of the sample volume did not influence the linearity, the sensibility or the reproducibility coefficient variation, once these values are in accordance with the ones defined by the protocol method procedure.

4.2 Measurements using the lab-on-a-chip

The electrical characterization and the performance of the on-chip detection and readout circuits were presented in ref. 18. Fig. 6 presents the spectral responsivity of two optical-channels measured when the detection chamber contains only the reagent. The ratio between the baseline and the peak maximum ranges from 4 to 10. The FWHM ranges from 4 to 8 nm. Any imperfection of the incident light wave and the roughness surface of the Fabry–Perot optical filter are responsible for the increased transmittance outside the narrow band to which the Fabry–Perot resonance cavity is tuned (the background signal). In addition, a compensation structure with the cavity optical length below $\lambda/10$ should be used. The transmittance signal of this structure is similar to the parasitic background and it is subtracted from the real signal. It should be mentioned that the conventionally used dark current

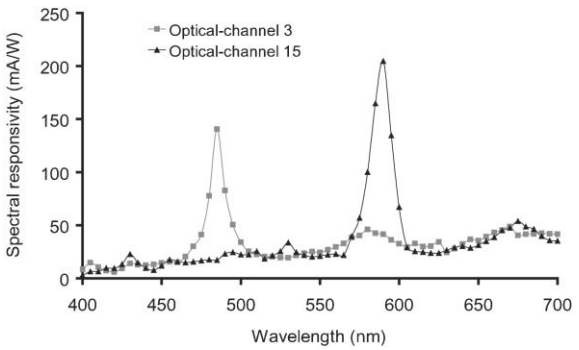

Fig. 6 Measured spectral responsivity of optical-channel 3 and 15, when the detection chamber contains only the reagent (optical effect of photodiode and optical filter included). The photodiode dark current is 2.03×10^{-18} A μm^{-2} at 0 V, its responsivity is 170 mA W^{-1} at $\lambda = 495$ nm and 223 mA W^{-1} at $\lambda = 592$ nm, and its sensitivity is 1 kHz Wm^{-2} at $\lambda = 670$ nm (measured using the TLS230 from Texas Instruments as reference). The light source was a 250 W quartz tungsten halogen lamp with the ORIEL Cornerstone 130™ monochromator.

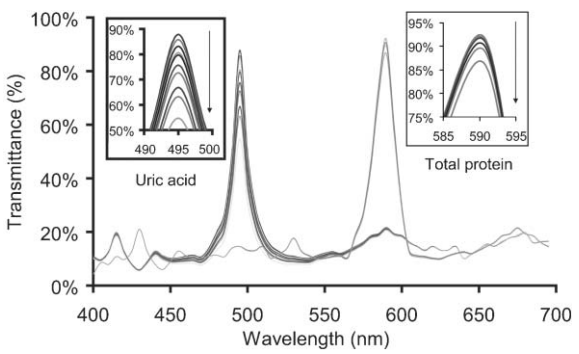

Fig. 7 Measured transmittance spectra for different uric acid and total protein concentrations (optical effect of photodiode and optical filter included). From top to bottom curves the analyte concentration increases. A 250 W quartz tungsten halogen lamp with the ORIEL Cornerstone 130™ monochromator was used as light source.

Table 3 Result of linear fit from absorbance calibration plot measured using the lab-on-a-chip and performed with a monochromatic light as light source

Analytes (measured conc. range/mg dl^{-1})	$\lambda_{(absorption\ maximum)}$/nm	Linear conc. range/mg dl^{-1}	Slope/(arb. units) dl mg^{-1}	Intercept (arb. units)	Correlation coefficient (R^2)
Uric acid (0–120)	495	0–30	$(2.1 \pm 0.4) \times 10^{-3}$	$(2 \pm 2) \times 10^{-3}$	0.98611
Total protein (0–100)	592	0–100	$(1.91 \pm 0.06) \times 10^{-4}$	$(-4 \pm 2) \times 10^{-4}$	0.99903

[a] Note: The $\pm$ values are $\pm$ one standard deviation.

Table 4 Result of linear fit from absorbance calibration plot measured using the lab-on-a-chip and performed with a white light as light source

Analytes (measured conc. range/mg dl^{-1})	$\lambda_{(absorption\ maximum)}$/nm	Linear conc. range/mg dl^{-1}	Slope/(arb. units) dl mg^{-1}	Intercept (arb. units)	Correlation coefficient (R^2)
Uric acid (0–120)	495	0–30	$(1.9 \pm 0.4) \times 10^{-3}$	$(3 \pm 2) \times 10^{-3}$	0.98016
Total protein (0–100)	592	0–100	$(1.9 \pm 0.2) \times 10^{-4}$	$(-0.5 \pm 2) \times 10^{-4}$	0.99665

[a] Note: The $\pm$ values are $\pm$ one standard deviation.

photodiode compensates only for the nonidealities of the detector itself. This method compensated for the nonidealities of the detector, Fabry–Perot filter and incident light, at the same time.

Fig. 7 shows the on-chip measured transmittance through the entire optical-channel for the same analytes, concentrations and procedures used in the measurements presented in section 4.1. The data are obtained using Lambert–Beer's law on the digitalized measured values of the transmitted light that reaches the photodetectors. It should be mentioned that the difference in the transmittance value for different total protein concentrations is small, which is due to the fact that human urine contains only small quantities of total protein, despite that its composition includes hundreds of proteins. The reproducibility mean coefficient variation of 10 replicate measurements for each uric acid concentration is less than 10% and for each total protein concentration is less than 15%. The resultant fit parameters are found in Table 3. With correlation coefficients above 0.986, the fit can be considered linear, although the data are not as good as the previous measurements due to the presence of the optical filter. Its presence limits the light transmitted to the underlying photodiode to less than 85% of the incident light. The Fabry–Perot optical filter performance could be increased by increasing the layers number of the dielectric mirrors, but the fabrication process complexity would also increase.

The spectral measurements on the lab-on-a-chip show that the optical-channels are sensitive to only one narrow spectral band centered at the wavelength for which the colored mixture has its absorption maximum, with a FWHM = 8 nm (see Fig. 7). These measurements, when compared with the ones without the optical filter, confirm that this optical filter can be used with a white light source for the lab-on-a-chip illumination, which makes the device portable. Moreover, the uric acid and the total protein concentration were measured, while illuminating the lab-on-a-chip with a 200 W halogen lamp source. The resultant fit parameters are found in Table 4. With correlation coefficients above 0.980, the fit can still be considered linear.

All the measurements on the lab-on-a-chip confirm the direct proportionality between intensity of the color produced by the mixture and the biomolecule concentration. The minimum detection of the lab-on-a-chip is 0.5 mg dl^{-1} and the achieved sensitivity is 5 mg dl^{-1} for both analytes, which corresponds to a relative resolution of 3.3%, enough for human being urine values. These results agree with macroscopic measurements performed with well-known uric acid and total protein standards and using state-of-the-art laboratory equipment.

5. Conclusions

The lab-on-a-chip presented here offers a new approach for clinical analyses, especially in biological fluids analysis, due to its portability, thus ensuring that the analysis can be performed at any location with instantaneous results. Moreover, the co-fabrication in a CMOS process of optical detection and filtering system avoids the need for expensive readout optics. In addition, the microfluidic system, fabricated using SU-8 techniques, features a low-cost disposable device, which avoids contamination between different analyses. The lab-on-a-chip performance was successfully demonstrated in the quantitative measurement of uric acid and total protein in human urine. However, other molecules or biological fluids are potential candidates for the lab-on-a-chip. Its highly selective filtering system makes the device broadly applicable, which would improve the use of spectrophotometric analysis in clinical diagnostics.

Acknowledgements

The authors wish to acknowledge Ger de Graaf and Peter Turmezei, both from the Department of Microelectronics of the Delft University of Technology, The Netherlands, for help with device fabrication and SU-8 processing, respectively. They also wish to acknowledge Paulo Freitas and Susana Freitas, from the INESC-MN, Portugal, for them help with the optical filter fabrication. This work was supported by the Portuguese Foundation of Science and Technology (FCT project SFRH/BD/1281/2000).

References

1 P. Connolly, *Biosens. Bioelectron.*, 1995, **10**, 1–6.
2 M. U. Kopp, H. J. Crabtree and A. Manz, *Curr. Opin. Chem. Biol.*, 1997, **1**, 410–419.

3 A. J. Tüdos, G. A. J. Besselink and R. B. M. Schasfoort, *Lab Chip*, 2001, **1**, 83–95.
4 J. C. Todd, A. H. Sanford and I. Davidsohn, *Clinical diagnosis and management*, 17th edn., W. B. Saunders Company, 1984.
5 *Biochemical and organic reagents*, 2002, Sigma-Aldrich.
6 S. K. Strasinger and M. S. Di Lorenzo, *Urianalysis and Body Fluids*, F. A. Davis, Company Press, Philadelphia, 2001.
7 http://www.hypoguard.com/diascreen_reagent_strips.html.
8 A. Manz, N. Graber and H. M. Widmer, *Sens. Actuators, B*, 1990, **1**, 244–248.
9 G. Minas, J. S. Martins and J. H. Correia, *Sens. Mater.*, 2002, **14**, 2, 77–89.
10 G. Minas, J. S. Martins, J. C. Ribeiro, R. F. Wolffenbuttel and J. H. Correia, *Sens. Actuators, A*, 2004, **110**, 33–38.
11 G. Minas, J. C. Ribeiro, R. F. Wolffenbuttel and J. H. Correia, *Proc. MME 2003*, ISBN: 90-808266-1-8, TUDelft, 2003, pp. 239–485.
12 H. A. Macleod, *Thin-film optical filters*, 3rd edn, Institute of Physics Publishing, 2001.
13 G. de Graaf and R. F. Wolffenbuttel, *Sens. Actuators, A*, 2004, **110**, 77–81.
14 SU-8: A Thin Photo-Resister for MEM's, http://aveclafaux.free-servers.com/SU-8.html.
15 http://www.inesc-mn.pt/listequip.htm.
16 P. Kabasakalian, S. Kalliney and A. Westcott, *Clin. Chem.*, 1973, **19**, 5, 522–524.
17 N. Watanabe, S. Kamel, A. Ohkubo, M. Yamanaka, S. Ohsawa, K. Makino and K. Tokuda, *Clin. Chem.*, 1986, **32**, 8, 1551–1554.
18 G. Minas, J. C. Ribeiro, G. de Graaf, R. F. Wolffenbuttel and J. H. Correia, *Proc. IEEE Sensors 2004*, ISBN: 0-7803-8692-2, IEEE, 2004, pp. 223–226.